

2015 SNMMI Highlights Lecture: Cardiovascular Nuclear and Molecular Imaging

Vasken Dilsizian, MD, University of Maryland School of Medicine, Baltimore, MD

From the Newsline Editor: The Highlights Lecture, presented at the closing session of each SNMMI Annual Meeting, was originated and presented for more than 30 years by Henry N. Wagner, Jr., MD. Beginning in 2010, the duties of summarizing selected significant presentations at the meeting were divided annually among 4 distinguished nuclear and molecular medicine subject matter experts. The 2015 Highlights Lectures were delivered on June 10 at the SNMMI Annual Meeting in Baltimore, MD. The first presentation is included here (the remaining lectures will appear in the October, November, and December Newsline issues). Vasken Dilsizian, MD, professor of Diagnostic Radiology and Nuclear Medicine and chief of the Division of Nuclear Medicine at the University of Maryland School of Medicine (Baltimore), spoke on cardiovascular nuclear and molecular imaging highlights from the meeting's sessions. Note that in the following presentation summary, numerals in brackets represent abstract numbers as published in The Journal of Nuclear Medicine (2014;57[*suppl 3*]).

Most of the cardiovascular-related abstracts presented at this meeting came from North America (64) and Asia (60), followed by Europe (37)—numbers quite similar to those at the 2014 meeting. Also similar this year is the fact that almost 3 times as many clinical abstracts were accepted for presentation as basic science abstracts. We are seeing a shift away from studies focusing on perfusion imaging, which still represents the majority of studies, to those on other areas of molecular imaging: atherosclerosis, innervation, infarction, vascular topics, sarcoidosis, and, new this year, infection and amyloidosis. The range of cardiovascular abstracts at this meeting also indicates that although almost 12,000 SPECT cameras and only about 2,500 PET cameras are currently in clinical use in the United States the science is clearly shifting toward PET and PET instrumentation. This year we also saw an increasing number of presentations on hybrid PET/MR techniques in cardiovascular imaging.

I would like to congratulate the first-place winner of the Cardiovascular Council Clinical Young Investigator Award, Christoph Rischpler, MD, from the Technische Universität München (Germany). Under the mentorship of Markus Schwaiger, MD, and Stephan Nekolla, PhD, he and his colleagues reported on “¹⁸F-FDG uptake in postischemic myocardium: relevance as a prognostic marker for functional recovery” [26]. This prospective study included 32 patients who presented with acute myocardial infarction and who underwent fasting heparin ¹⁸F-FDG PET/MR imaging 4.9 ± 1.3 days after acute angioplasty. The researchers compared PET biosignal assessment of inflammatory markers with early MR

measures of acute inflammatory response and with delayed-enhanced MR measures of interstitial fibrosis. Of interest was the potential prognostic value of ¹⁸F-FDG PET for functional outcomes after myocardial infarction. Figure 1 is an example from a patient who presented with inferior-lateral hypoperfusion on acute sestamibi imaging (left). The MR image (middle) shows delayed gadolinium enhancement in the same region, and PET (right) shows high activity in the area of acute injury. The researchers asked whether perfusion reflects and/or predicts increased inflammatory response and functional recovery. They found a linear correlation between summed ¹⁸F-FDG activity scores and those from delayed-enhancement MR imaging, although overall the extent of ¹⁸F-FDG uptake was larger (defining a larger area of risk) than that of gadolinium on late enhancement. Interestingly enough, an inverse relationship between the extent of ¹⁸F-FDG uptake in the infarct territory and change in ejection fraction was observed, reflecting improvement after reperfusion therapy. Given the fact that ¹⁸F-FDG is taken up by the myocytes as well as inflammatory cells, it would be quite difficult to definitively identify inflammatory activity and differentiate the signal from background myocardial ¹⁸F-FDG uptake, something these authors acknowledge. We have already seen in the published literature that acute ischemia on the treadmill is associated with an immediate shift of metabolism from fatty acid to glucose, with imaging showing hypoperfused myocardial regions with increased glucose utilization. This switch in metabolism can persist up to 30 hours after the ischemic event, a phenomenon we have described as metabolic stunning, also known as ischemic memory.

MR imaging offers superior elucidation of morphology in plaque lesions and carries the advantage of reducing the patient’s exposure to radiation. Li et al. from the Medical University of Vienna (Austria) reported on “Quantitative assessment of ¹⁸F-FDG PET/MRI in atherosclerotic plaque: comparison to PET/CT hybrid system” [187]. These authors looked at 27 oncology patients and measured ¹⁸F-FDG uptake on PET/MR and PET/CT imaging, with a focus on correlations between quantitative measures of maximum standardized uptake values (SUV_{max}) and maximum target-to-blood ratios (TBR_{max}). They showed that although overall mean SUV_{max} tended to be lower with PET/MR than PET/CT imaging, these values were correlated, with an



Vasken Dilsizian, MD

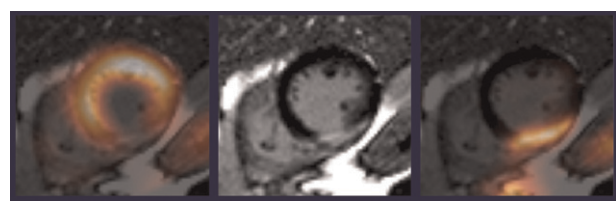


FIGURE 1. ^{18}F -FDG PET and MR after acute angioplasty. Images from patient who presented with inferior-lateral hypoperfusion on acute sestamibi imaging (left). Late MR image (middle) shows delayed gadolinium enhancement in same region, and ^{18}F -FDG PET shows high activity in area of acute injury (right).

r value of 0.65. The correlation of TBR_{max} values between the 2 imaging modalities was significantly better, with an r value of 0.85 (Fig. 2).

A key paper presented at the SNMMI meeting focused on coronary artery disease (CAD) outcomes data, relating the severity of ischemia to complete revascularization. Li et al. from the State Key Laboratory of Cardiovascular Disease, Fuwai Hospital, National Center for Cardiovascular Diseases, Chinese Academy of Medical Sciences, and Peking Union Medical College (Beijing, China) reported on “Outcomes of CAD patients treated by complete and incomplete revascularization and medical therapy” [239]. This group looked at 286 consecutive patients with abnormal angiography and myocardial ischemia on SPECT and followed these patients for 45 ± 21 months. Factors assessed included death and major adverse cardiac events in relation to the extent and severity of myocardial ischemia (categorized as mild-to-moderate or severe) and revascularization (categorized as complete or incomplete) or medical therapy. On analysis of results for severe ischemia, the authors identified marked improvement in survival in those who had complete revascularization compared with those who were on medical therapy or who had incomplete revascularization. In contrast, results for mild-to-moderate ischemia did not show significant survival differences between those who underwent revascularization and those who had incomplete revascularization or medical therapy. This is a very timely study, because in 2012 the National Heart, Lung, and Blood Institute launched the International Study of Comparative Health Effectiveness with Medical and Invasive Approaches (ISCHEMIA) trial, a prospective, randomized, clinical study designed to determine the best management strategy for higher-risk patients with stable ischemic heart disease. This trial will enroll 8,000 patients by 2019, and it will be interesting to see whether the results of this multicenter prospective effort mirror the findings of the single-center CAD study presented at the SNMMI meeting.

Molecular Imaging: Beyond Perfusion

Other areas that were investigated and reported on at the meeting included myocardial infarction, myocardial innervation, vulnerable plaque imaging, cardiac amyloidosis, cardiac device infection, and thrombus imaging, each of which

will be represented in this overview by a single example selected from among many outstanding presentations. The first-place winner of the Cardiovascular Council Basic Young Investigator Award was Junaid Afzal, PhD, from Johns Hopkins University (Baltimore, MD). Afzal and colleagues reported that “Dual isotope SPECT-CT imaging using sodium-iodide symporter (NIS) reveals improved energetics following cardiac transplantation of stem cells encapsulated in hydrogels” [22]. They noted that cell suspension prior to transplantation typically results in depressed cellular energetics and low engraftment. To address this problem, they designed hydrogels that promote cell adhesion, restore metabolism, and boost engraftment. They conducted *in vivo* and *in vitro* studies of cell metabolism in cardiosphere-derived stem cells and used NIS as a reporter to visualize and track the cells. Cells were imaged with dual-isotope (^{201}Tl , $^{99\text{m}}\text{Tc}$) SPECT/CT at 1 and 24 hours after transplantation. The researchers also applied reversible inhibition of Akt (protein kinase B) using MK2205 to investigate hydrogel-mediated restoration of metabolism. They found that hydrogel encapsulation rapidly increased metabolism of epicardial transplanted stem cells by activating Akt and that *in vivo* dual-isotope SPECT/CT imaging documented this process (Fig. 3). For suspended NIS plus stem cells and intramyocardial transplantation, little or no tracer uptake was seen in early (1–3-hour) or later (24-hour) images. In contrast, when hydrogel-encapsulated cells were implanted epicardially, intense activity was seen both early and at 24 hours. Although these findings are encouraging, it would be important to implant these cells within the myocardium and determine whether improvements in function or physiologic uptake would follow.

Cardiac Innervation

Another area of current interest in cardiology is cardiac innervation. ^{123}I -metaiodobenzylguanidine (^{123}I -MIBG) is now approved for imaging of cardiac innervation. Most

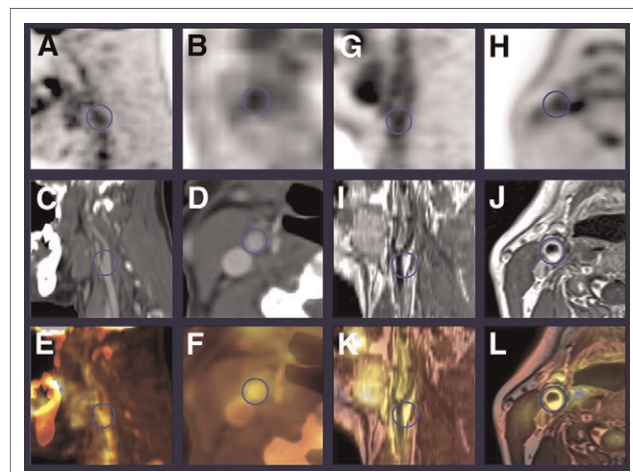


FIGURE 2. PET/MR was found to offer superior morphology/conspicuity of plaque lesions at reduced radiation dose. PET/CT (A-F): sagittal (A,C,E); transverse (B,D,F); PET (A,B); CT (C,D); fused PET/CT (E,F). PET/MR (G-L): sagittal (G,I,K); transverse (H,J,L); PET (G,H); MR (I,J); fused PET/CT (K,L).

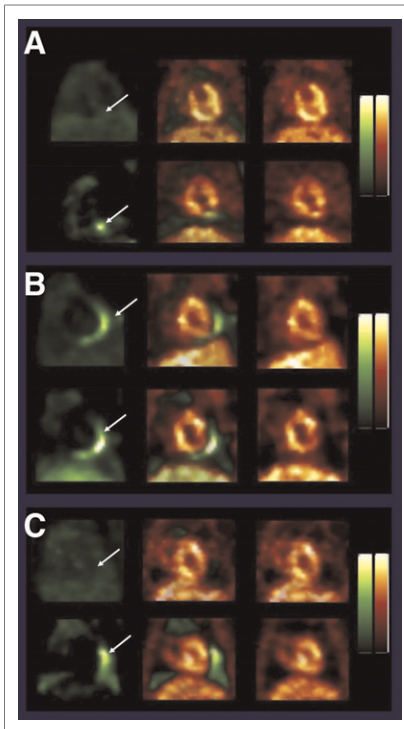


FIGURE 3. Dual-isotope SPECT/CT imaging of cardiac-derived stem cell (CDC) transplantation (left to right in each block, ^{99m}Tc SPECT/CT, fused $^{99m}\text{Tc}/^{201}\text{Tl}$ SPECT/CT, and ^{201}Tl SPECT/CT images). For suspended NIS CDCs and intramyocardial transplantation, little or no tracer uptake was seen in early (A, 1–3 hours) or later (C 24 hours) images. In contrast, when these NIS CDCs were hydrogel-encapsulated and implanted epicardially, activity was seen both early and at 24 hours (B). Additional MK2206 retreatment for reversible Akt inhibition

in these hydrogel-encapsulated CDCs resulted in further enhancement (right).

innervation imaging is performed with planar imaging to assess the heart-to-mediastinal ratio, and, in most instance, planar and SPECT imaging is limited by relatively poor counts. A PET radiotracer, particularly one that is ^{18}F labeled and therefore clinically available, would be welcome. Lapa et al. from University Hospital Würzburg (Germany) and Lantheus Medical Imaging (North Billerica, MA) reported on “In-vivo kinetics of the sympathetic PET tracer $^{18}\text{F-LMI1195}$ ” [518]. These investigators looked at a new tracer, $^{18}\text{F-LMI1195}$, and compared its effectiveness with the currently available tracer ^{11}C -metahydroxyephedrine ($^{11}\text{C-HED}$). They noted that $^{11}\text{C-HED}$ retention is maintained by continuous uptake and release at the nerve terminal, whereas $^{18}\text{F-LMI1195}$ retention in the vesicular storage may more closely mimic physiologic norepinephrine turnover. Studies were conducted in 3 medication groups in animals: (1) a control group; (2) a group with desipramine (a neuroepinephrine transporter inhibitor) chase 10 minutes after tracer injection;

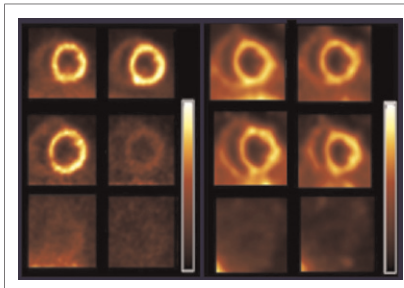


FIGURE 4. $^{11}\text{C-HED}$ (left block) vs $^{18}\text{F-LMI1195}$ (right block) PET myocardial innervation. Top rows: controls; middle rows: desipramine chase; bottom rows: desipramine plus pretreatment with reserpine.

and (3) desipramine plus pretreatment with reserpine (a vesicular transport blockade inhibitor) (Fig. 4). With $^{11}\text{C-HED}$ and the desipramine chase the activity washed out. In contrast, the chase with the $^{18}\text{F-LMI1195}$ made no difference in washout and the tracer was maintained in the vesicular region. Again, additional studies will be needed to determine whether this agent will better mimic norepinephrine turnover in human heart failure models, but an ^{18}F -labeled PET radiotracer that looks at innervation is promising.

Atherosclerosis and Plaque Imaging

A major focus of coronary medicine is to identify and accurately diagnose patients who present with acute coronary syndrome or vulnerable plaque rupture. At this meeting a number of reports described agents used to look at various aspects of vulnerable plaque and its characteristic pathologic features. These agents targeted microcalcification ($^{18}\text{F-NaF}$), apoptosis (^{99m}Tc -gold nanoparticles, Annexin V, $^{18}\text{F-ML-10}$), angiogenesis ($^{64}\text{Cu-NOTA-3-4A}$), and hypoxia ($^{64}\text{Cu-diacyl-bis-4-methylthiosemicarbazone}$). $^{18}\text{F-NaF}$ is clinically available for microcalcification imaging. In 2014 Joshi et al. reported in the *Lancet* (2014;383:705–713) on the use of $^{18}\text{F-NaF}$ in patients presenting with acute coronary syndrome and published images of microcalcifications and carotid plaque rupture. They demonstrated that $^{18}\text{F-NaF}$ appears to be better than $^{18}\text{F-FDG}$ in identifying vulnerable plaques. This is not really surprising, because background myocardial $^{18}\text{F-FDG}$ uptake can interfere with the signal of the $^{18}\text{F-FDG}$ within coronary plaque inflammation, whereas $^{18}\text{F-NaF}$ provides a much stronger signal-to-background ratio because it localizes only in the areas of active microcalcification in the thin fibrous cap of the atherosclerotic plaque and not in the myocardium.

At the SNMMI meeting, Rubeaux et al. from Cedars-Sinai Medical Center (Los Angeles, CA) and the University of Edinburgh (UK) reported on “Motion-frozen

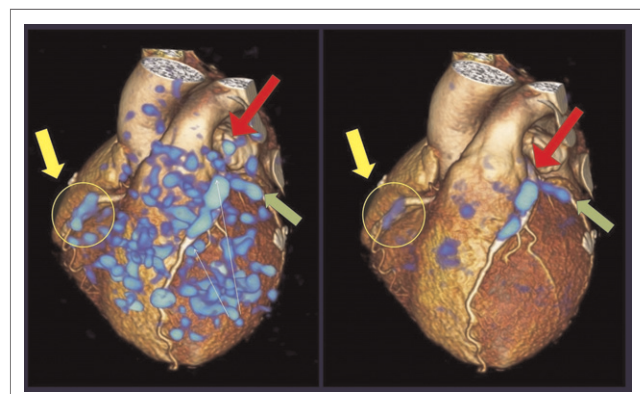


FIGURE 5. Reduction of noise and signal increase with “motion frozen” ^{18}F -sodium fluoride PET. Patient with multivessel CAD with vulnerable plaques. In non-motion corrected image (left), blue areas represent noise that obscures ^{18}F -sodium fluoride signal in right coronary artery, left anterior descending artery, and left circumflex territory. With “motion frozen” technique (right), noise is significantly reduced and activity in coronary vessels is clearly visualized.

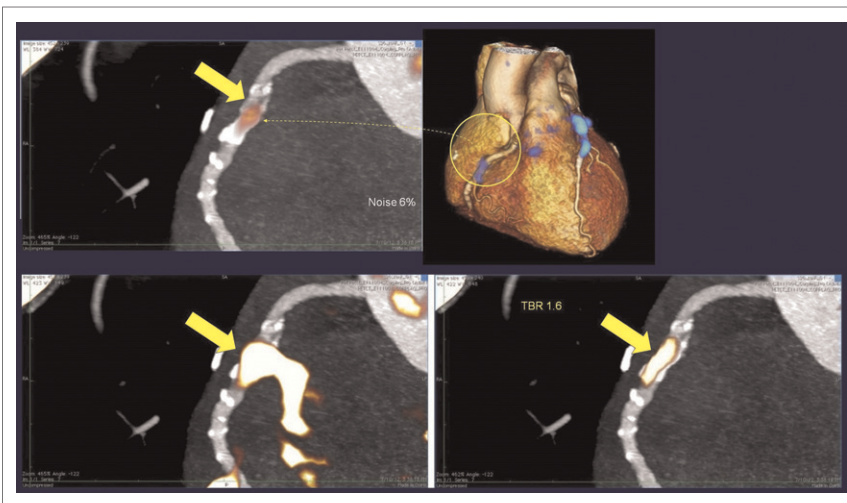


FIGURE 6. Increase in target-to-blood ratio with “motion frozen” ^{18}F -sodium fluoride PET. In nongated image with noise at 6%, target-to-blood ratio was 1.4 (top left); with 1-gated PET it was 1.5 (bottom left); and when all gates with motion-frozen technique were applied it was 1.6 (bottom right).

^{18}F -sodium fluoride PET for imaging coronary atherosclerotic plaques” [79]. These researchers took imaging data from the original *Lancet* study and attempted to quantify vulnerable plaque by addressing the problem of coronary artery motion. They introduced a “motion frozen” technique of gated coronary PET/CT and applied it in imaging data from 17 patients (51 lesions). With this technique, noise was reduced by ~50% compared with 1-gate PET imaging. The technique also increased TBRs by

motion-frozen technique is promising for improvement in motion correction and noise.

With CT angiography, we are really looking at vascular wall calcification, which represents advanced, late stages of stable atherosclerotic plaque with morphologic calcium deposits. Plaque formation, however, represents progressive disease, with perhaps the earliest sign being inflammation, followed by ongoing active microcalcification. Salavati et al. from the University of Pennsylvania (Philadelphia, PA) and

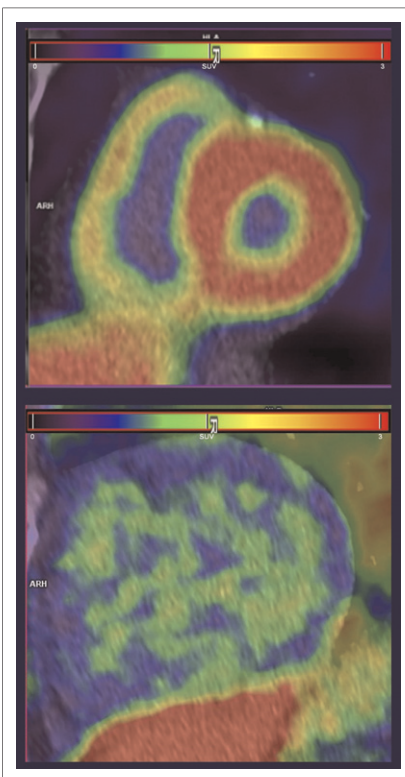


FIGURE 7. ^{11}C -PiB PET in AL cardiac amyloidosis. Top: positive image; bottom: negative image.

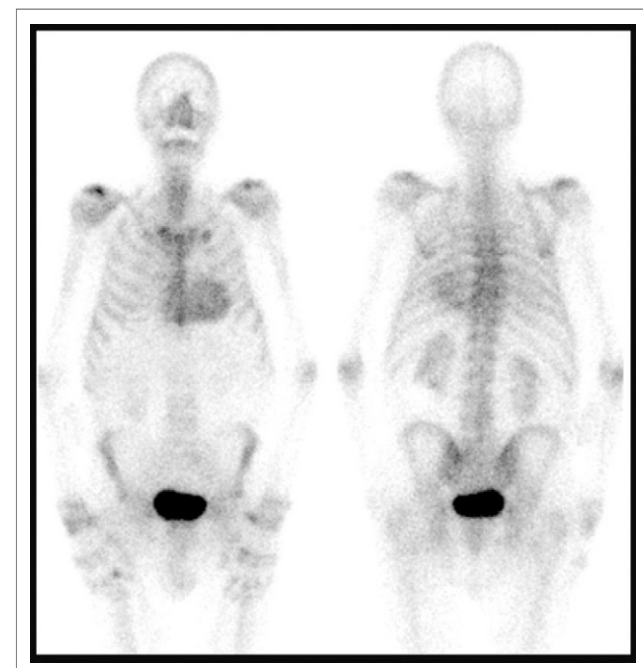


FIGURE 8. $^{99\text{m}}\text{Tc}$ -HMDP myocardial scintigraphy in transthyretin-type amyloidosis. Left image shows tracer uptake in heart. Analysis of heart-to-skull ratios for tracer retention proved to be predictive of major adverse cardiac event survival.

~33% compared with 1-gate PET imaging. Figure 5 is a nice example of multivessel CAD with vulnerable plaques. In the non-motion corrected image (left), the blue areas represent noise that obscures the ^{18}F -sodium fluoride signal in the right coronary artery, the left anterior descending artery, and the circumflex territory. With the “motion frozen” technique (right) the noise is significantly reduced and the activity in the coronary vessels is clearly visualized. In a nongated image with noise at 6% the TBR was 1.4, with 1-gated PET it was 1.5, and, when all gates were applied with the motion-frozen technique, the TBR increased to 1.6 (Fig. 6). This ability to clearly quantitate ^{18}F -NaF in cardiac imaging moves the field beyond visual assessment alone, and motion-

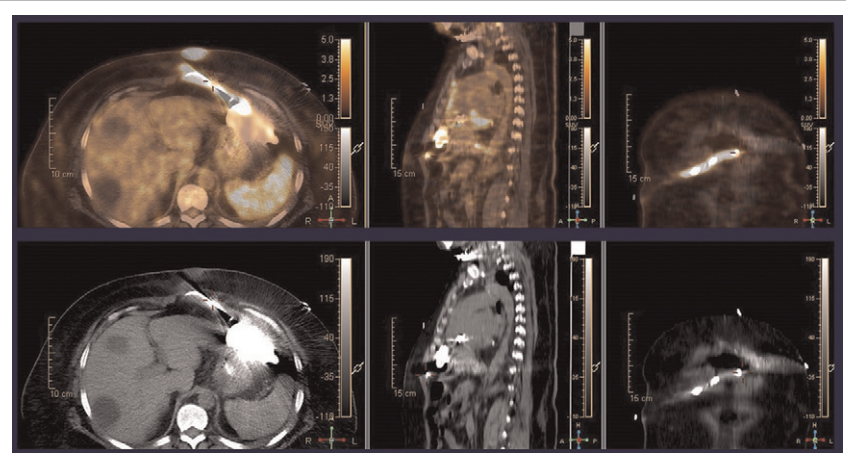


FIGURE 9. ^{18}F -FDG PET imaging of implant infection in LVAD driveline exit site, representing peripheral site. PET/CT images show linear area of increased metabolic activity along the driveline and percutaneous exit in the abdominal wall. Note importance of reviewing non-attenuation corrected images.

Indiana University School of Medicine (Indianapolis) reported on “Assessment of ^{18}F -NaF PET/CT as a diagnostic tool for early detection of coronary artery calcification” [460]. These investigators wanted to determine whether it was possible to use ^{18}F -NaF PET/CT to identify microcalcifications in a swine model of metabolic syndrome when macroscopic evidence of calcification was not evident. They compared imaging results in 11 swine with metabolic syndrome and 3 lean control animals and showed an almost 2-fold increase in ^{18}F -NaF uptake in the coronaries and 2.5-fold increase in global molecular microcalcium score in the metabolic syndrome animals. Although intravascular ultrasound lesion assessment in the metabolic syndrome group showed 5-fold greater neointimal wall coverage than that observed in lean swine, this technique identified a focal macroscopic calcified lesion in only 1 metabolic syndrome swine. Agatston

public of Korea) reported on “Diagnostic and prognostic implication of ^{11}C -Pittsburgh B positron emission tomography in AL cardiac amyloidosis” [25]. They used ^{11}C -PiB PET in 22 chemotherapy-naïve patients who had been diagnosed with monoclonal light-chain cardiac amyloidosis by either endomyocardial biopsy or echocardiography criteria. The patients were followed for clinically significant events, including death and admission for heart failure. Imaging was positive in 16 patients and negative in 6 patients (Fig. 7). During 3-year follow-up, 12 of the 22 patients died. Of these 12, 11 had been positive on early ^{11}C -PiB PET imaging. This tracer may have significant utility beyond assessment of Alzheimer disease.

One group at the SNMMI meeting presented an alternative way of looking at amyloidosis by using the already long-established bone-scanning agent $^{99\text{m}}\text{Tc}$ -hydroxymethylene diphosphonate ($^{99\text{m}}\text{Tc}$ -HMDP). Van Der Gucht et al. from the Henri Mondor Hospital (Créteil, France) reported that “ $^{99\text{m}}\text{Tc}$ HMDP myocardial scintigraphy is predictive of major adverse cardiac event (MACE) in patients with transthyretin-type (TTR) amyloidosis” [27]. Among 55 TTR amyloidosis patients, heart-to-skull retention was correlated with cardiac amyloidosis severity (left ventricular ejection fraction and N-terminal of the prohormone brain natriuretic peptide). Patients were followed for a median of 11 days (range, 50–343 days). Figure 8 (left) shows uptake of radiotracer in the heart. Quantitative analysis of heart-to-skull ratios for tracer retention showed that patients with lower heart-to-skull scores experienced better survival rates. When the authors added in New York Heart

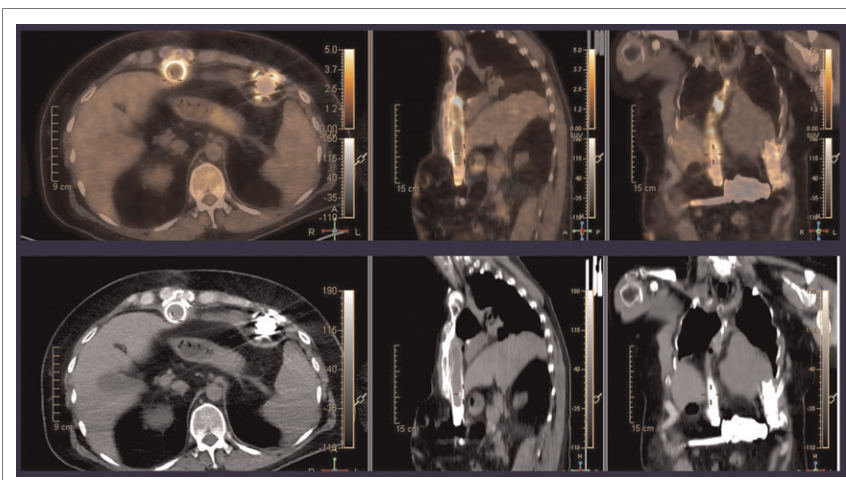


FIGURE 10. ^{18}F -FDG PET imaging of implant infection in LVAD cannula outflow tract, representing central site. PET/CT images show intense linear metabolic activity along outflow cannula exterior attached to ascending aorta. Note importance of reviewing non-attenuation corrected images.

CT calcium scores were 0 in all animals. ^{18}F -NaF PET/CT, then, provides another potential tool for identifying microcalcifications in the early stages of atherosclerotic plaque and their vulnerability to rupture, long before macroscopic evidence of calcification is seen on CT.

We have all seen the advances in neurosciences that are underway with the advent of amyloid imaging of plaque in the brain. Three agents are currently U.S. Food and Drug Administration approved, and these are waiting for resolution of Centers for Medicare & Medicaid Services reimbursement. One of these is ^{11}C -Pittsburgh B (^{11}C -PiB), and early evidence suggests that this tracer may have beneficial applications in cardiac amyloidosis. Lee et al. from Seoul National University Hospital (Re-

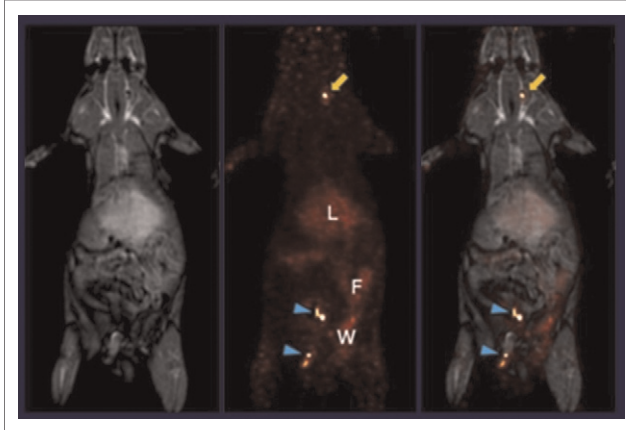


FIGURE 11. Whole-body, multisite thrombus detection with ^{64}Cu -FBP8 PET/MR imaging. MR, left; PET, middle; fused PET/MR, right. Thrombus is clearly seen in right carotid artery and right femoral vein.

Association classifications to the analysis, they were able to further stratify patients beyond the amyloid signal, suggesting that this technique could be used clinically to predict outcomes and change management.

Cardiac Device Infection

At the University of Maryland School of Medicine, we have been interested in using ^{18}F -FDG for evaluation of cardiac device infection for quite some time. We have used this clinically for identifying infection at both the pocket and the wire in cardiovascular implantable electronic devices and also in prosthetic valve infections. Jongho Kim, MD, and colleagues from our group reported that “The presence and site of left ventricular assist device (LVAD) infection by FDG PET/CT bears important prognostic implications” [310]. The study included 35 patients with heart failure and suspected infection in LVAD implants. All underwent ^{18}F -FDG PET/CT imaging, and findings were compared with microbiologic data and/or clinical follow-up. Twenty-seven patients showed LVAD infection on imaging and 8 did not, numbers confirmed at microbi-

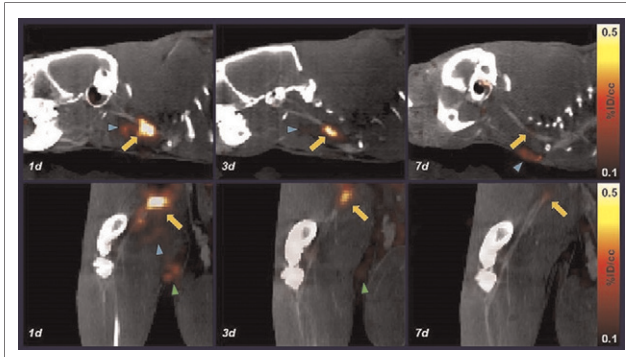


FIGURE 12. Age-dependent changes in thrombus uptake with ^{64}Cu -FBP8 PET/MR. Arterial (top row) and venous (bottom row) thrombus uptake on days 1, 3, and 7 (left to right), showing that thrombus uptake was higher when the clot was younger and fibrin rich than when it was older.

ology and follow-up. Twelve of the 27 patients with infection died of cardiac causes over the course of the 2-year follow-up. Those with infection at central sites (cannula or pump) had significantly poorer prognoses than those with infection at more peripheral sites (exit sites or drivelines). These findings suggest that ^{18}F -FDG PET/CT is a useful technique not only for localizing the site of LVAD infection but for identifying high-risk patients with infection (Figs. 9 and 10).

Thrombus Imaging

Blasi et al from the Massachusetts General Hospital (Boston, MA) reported that “Molecular imaging of thrombosis using FBP8-PET allows whole-body thrombus detection and fibrin content estimation” [78]. These investigators worked with ^{64}Cu -FBP8, a small peptide-based probe with high specificity for fibrin. Thrombosis is often the underlying cause of major cardiovascular disease, including heart attack, stroke, and venous thromboembolism, and is one of the leading causes of morbidity and mortality. To have a probe that is PET based and that could characterize thrombosis with high sensitivity would be a welcome addition to our imaging armamentarium. These researchers induced thrombosis with a ferric chloride application on the carotid artery and femoral vein in 30 Sprague–Dawley rats. ^{64}Cu -FBP8 PET was performed at 1, 3, and 7 days after thrombus induction to determine whether thrombus could be visualized and to assess how the signal would change. The whole-body thrombus detection capabilities of ^{64}Cu -FBP8 PET were further assessed in a rat model of deep vein thrombosis and pulmonary embolism. Figure 11 is a whole-body PET/MR image acquired 1 hour after ^{64}Cu -FBP8 injection. Thrombus is clearly seen in

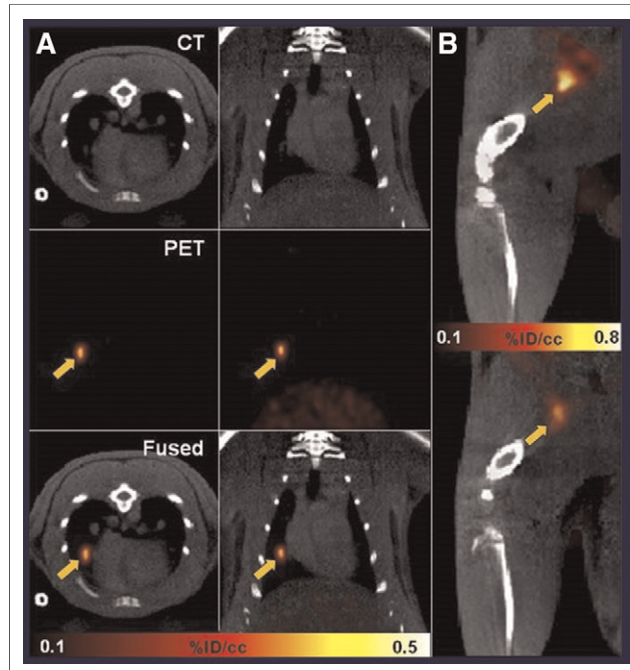


FIGURE 13. ^{64}Cu -FBP8 PET/MR thrombus imaging. Both deep venous thrombosis and a pulmonary embolism (arrow) could be identified with a single probe injection.

the right carotid artery and the right femoral vein. They also applied this technique to look at differences in thrombus uptake depending on time of imaging (Fig. 12). They showed both arterial and venous thrombus uptake on days 1, 3, and 7, finding that in both arterial and venous thrombus uptake was higher when the clot was younger and fibrin rich than when it was older. In some instances, both deep venous thrombosis and a pulmonary embolism could be identified with a single probe injection (Fig. 13). Given the percentage of patients with deep venous thrombosis who develop pulmonary emboli, this could be an extraordinarily valuable tracer once clinically validated.

Conclusion

I would like to congratulate all the investigators who participated in this year's SNMMI cardiovascular scientific sessions, working together for a shared goal of providing state-of-the-art care to our patients and advancing medical science and molecular imaging by teaching and learning from each other. I would also like to extend a special acknowledgment to my colleague Wengen Chen, MD, PhD, who, as an intern on the Cardiovascular Council for 2 years in a row, assisted me by obtaining these summary slides from investigators in preparation for these talks.

Nuclear Medicine, Social Media, and Two Degrees of Separation

George Segall, , MD, Executive Director, American Board of Nuclear Medicine

The American Board of Nuclear Medicine (ABNM) is one of the smaller boards among the 24 member boards of the American Board of Medical Specialties (ABMS). The ABNM has certified 5,600 physicians since the first certification examination in 1972 and currently has more than 4,700 active diplomates. Approximately 60–80 new diplomates are certified each year, a steady number for the last 4 decades. In comparison, the 3 largest medical boards have each certified more than 100,000 physicians and collectively account for approximately half of the nearly 1 million physicians certified by ABMS member boards.

One of the unique attributes of our small medical and scientific community is the personal connection we have with one another. Six degrees of separation is a theory postulated by Hungarian author Frigyes Karinthy in 1929, asserting that everyone can be connected to any other individual through no more than 5 people. World population was estimated to be 2 billion people in 1927.

How closely are we connected with one another in our medical and scientific community? To help answer that question, I asked 2 colleagues to separately identify 10 individuals who have advanced nuclear medicine. The list included physicians as well as scientists in the United States and abroad. Four individuals were included in both lists, for a total of 16 luminaries. I wrote to each of these 16 individuals and asked him or her to indicate those on the list with whom they had a professional connection, including a minimum of 1 face-to-face conversation or meeting. I received answers from 12 individuals, who indicated they had a direct professional connection (0 degrees of separation) with a remarkable average of 70% of the other individuals on the list (range 33%–100%). Based on this admittedly nonscientific survey, one could reasonably estimate that we are all professionally connected to one another with no more than 2 degrees of separation.

The nuclear medicine community in the United States has 1 leading professional society, SNMMI, in addition to several other professional organizations that significantly contribute to education and research. SNMMI membership in 2015 is more than 18,000, including more than 14,000 technologists, 2,622 physicians, and 885 scientists and pharmacists. A large number of nuclear medicine professionals attend the annual meeting, which provides an opportunity for making new professional connections. Approximately 1,739 physician members (66%) attended at least 1 annual meeting from 2011 to 2015.

Digital social networks are becoming a large part of everyday life as a result of convenience and universal connection to the Internet. The ABNM made its debut on social media in September 2014. You can find us on Facebook at <https://www.facebook.com/americanboardofnuclearmedicine>, on Twitter @ABNM or <https://twitter.com/ABNM>, or you can search ABNM on either site. Both sites contain important dates and updates regarding examinations, as well as other useful information. Social media allows the ABNM to share information with diplomates between semiannual newsletters and, more important, allows individuals to communicate with one another as well as with the board.

Our professional connections are the bedrock of the nuclear medicine community. The personal and digital network that we have created is a tangible asset that helps us advance professionally and scientifically. Many challenges and opportunities lie ahead. We will meet them together.



George Segall, MD